

Energy Conversion and Management
Manuscript Draft

Manuscript Number: ECM-D-15-01631

Title: Thermal efficiency of coal based power plants: from theoretical to practical assessments

Article Type: Original research paper

Section/Category: 6. Fuels, Combustion, and Chemical Processes

Keywords: coal based power plant; benchmarking; exergy analysis; CO₂ capture

Abstract: The improvement in thermal efficiency for coal to power processes is increasingly important due to concerns on CO₂ emissions. This paper presents a systematic study on direct combustion coal to power processes with respect to thermodynamic, technical and economic factors. Traditional exergy analysis focuses on irreversibilities in existing processes, while the new methodology investigates the thermal efficiency from its theoretical maximum to practical values by adding irreversibilities one by one. As a result of the study presented in this paper, various measures for increasing the thermal efficiency are investigated and the corresponding improvement potential is presented. For a reference power plant, the exergy of the coal feed is calculated to be 1.08 times the lower heating value, while the actual thermal efficiency is 45.5% when irreversibilities for the combustion reaction, the heat transfer between flue gas and water/ steam, the low temperature heat losses, the steam cycle, and other factors are included. Different measures to increase the thermal efficiency of the reference plant by 0.1% points are presented. The minimum thermal efficiency penalty related to CO₂ capture is 2.92-3.49% points within an air factor range of 1.0-1.4 when the CO₂ is 100% recovered.

1 Thermal efficiency of coal based power plants: 2 from theoretical to practical assessments

3
4 *Chao Fu^{a*}, Rahul Anantharaman^b, Kristin Jordal^b, Truls Gundersen^a*

5
6 ^a Department of Energy and Process Engineering, Norwegian University of Science and
7 Technology, Kolbjorn Hejes v. 1A, NO-7491 Trondheim, Norway

8 ^b SINTEF Energy Research, Kolbjorn Hejes v. 1A, NO-7491 Trondheim, Norway

9 * Corresponding author. Tel.: +47 73592799; E-mail address: chao.fu@ntnu.no

10 **Abstract**

11 The improvement in thermal efficiency for coal to power processes is increasingly important
12 due to concerns on CO₂ emissions. This paper presents a systematic study on direct
13 combustion coal to power processes with respect to thermodynamic, technical and economic
14 factors. Traditional exergy analysis focuses on irreversibilities in existing processes, while the
15 new methodology investigates the thermal efficiency from its theoretical maximum to
16 practical values by adding irreversibilities one by one. As a result of the study presented in
17 this paper, various measures for increasing the thermal efficiency are investigated and the
18 corresponding improvement potential is presented. For a reference power plant, the exergy of
19 the coal feed is calculated to be 1.08 times the lower heating value, while the actual thermal
20 efficiency is 45.5% when irreversibilities for the combustion reaction, the heat transfer
21 between flue gas and water/ steam, the low temperature heat losses, the steam cycle, and other

22 factors are included. Different measures to increase the thermal efficiency of the reference
23 plant by 0.1% points are presented. The minimum thermal efficiency penalty related to CO₂
24 capture is 2.92-3.49% points within an air factor range of 1.0-1.4 when the CO₂ is 100%
25 recovered.

26 **Keywords:** coal based power plant; benchmarking; exergy analysis; CO₂ capture.

27 **1. Introduction**

28 Coal will continue to be a dominant energy source also in the next decades. It was responsible
29 for 41% of the world power generation in 2012 and is projected to be around 31% in 2040[1].
30 Coal based power plants have been developed for more than 100 years with respect to the
31 capacity and thermal efficiency. The plant thermal efficiency has increased continuously from
32 around 5% to 45% in the past century[2]. Reducing cost for power generation has always
33 been a motivation for efficiency improvement. The increasing concerns about CO₂ emissions
34 stimulate further improvements in thermal efficiency. In direct combustion coal to power
35 processes, the chemical energy of coal is converted into heat and this heat is further converted
36 into power. Considerable efforts have been made to improve the thermal efficiency, such as
37 reducing the irreversibilities in the process that converts the chemical energy of coal into
38 heat[3], maximizing power production from the heat[4] and minimizing the losses of low
39 temperature heat[5]. For pulverized coal based power plants, the long-term target on thermal
40 efficiency is above 55% by using steam with maximum temperatures around 1073 K
41 (800°C)[5].

42 The thermodynamic principles of coal based power plants (mainly steam cycles) have been
43 described in many textbooks related to thermodynamics and power technologies[5-10].

44 Various measures for improving the plant performance have also been presented in these
45 books as well as in many other publications. The primary objective of this paper is to

46 investigate the improvement potential in thermal efficiency and the corresponding limitations
47 for such measures presented in literature. The paper is an extension of the work by Fu et
48 al.[11]. The study starts by calculating the maximum thermal efficiency for a specific coal feed
49 in an ideal (reversible) power plant. This efficiency will decrease when realistic (irreversible)
50 unit operations are added for the combustion process, the heat transfer process, the steam
51 cycle, and the flue gas treatment (CO₂ emission control). The thermodynamic losses
52 (irreversibilities) are caused by spontaneous processes such as combustion, as well as heat
53 transfer at finite (often large) temperature differences, mixing, pressure drops, and turbo-
54 machinery inefficiencies. In addition, the thermal efficiency is limited by technical and
55 economic factors, such as excess air for combustion, maximum pressure and temperature of
56 the main steam, and low temperature heat losses. The influence of these limiting factors on
57 the thermal efficiency has been investigated. For the reference plant, the measures for
58 increasing the thermal efficiency by 0.1% points are investigated. The minimum energy
59 penalty with respect to thermodynamic limitations for capturing CO₂ at various purities and
60 recovery rates is also studied. The results can be used as a basis for evaluating the thermal
61 efficiency of plants where CO₂ capture will be implemented in the future, and also the
62 efficiency improvement measures.

63

64 **2. Methodology**

65 A methodology for benchmarking and identifying improvement potentials of processes was
66 presented by Anantharaman et al.[12]. The motivation for the new methodology was to
67 develop a systematic and consistent way to identify improvement potential and integration
68 opportunities in power processes with CO₂ capture. To this end, three efficiencies that can be
69 specified for a process are[12]:

70 (1) Thermodynamics limited: This is a scheme that requires the thermodynamically lowest
71 possible energy input to produce the specified energy output. The resulting efficiency is the
72 "ideal" efficiency that is the thermodynamically maximum attainable for such a process.
73 This efficiency can never be achieved in practice since it requires perfectly reversible
74 processes, however, it provides a thermodynamic benchmark or target for process design.

75 (2) Technology limited: Limitations, both technological and those inherent in unit
76 operations, prevent achieving the thermodynamic maximum efficiency. The thermal
77 efficiency attainable by employing state-of-the-art technology can be thought of as a
78 technology limited efficiency, which is typically compared in different benchmarking
79 studies[13].

80 (3) Economics limited: While the technology limited efficiency by definition is achievable,
81 it may not necessarily be economical. Latest technologies are often associated with a
82 premium, which makes utilizing them economically infeasible. Thus the economics limited
83 efficiency is the efficiency of a process using technology that results in a process that is
84 commercially viable.

85 Power plants with CO₂ capture can be benchmarked with respect to the three above-
86 mentioned efficiencies. It must be noted that while the thermodynamic limited efficiency is
87 fixed for a given process, the technology limited and economics limited efficiencies are
88 subject to change over time. The difference between the thermodynamic maximum and the
89 technology limited efficiencies quantifies the theoretical improvement potential and
90 constitutes an additional source of information for benchmarking studies, which merits further
91 attention. The source(s) of this difference in efficiency can point to possible future directions
92 for technology development.

93 The approach in this paper consists of applying engineering thermodynamics to increase the
94 understanding of the fundamental losses imposed on a power cycle. The first step in the
95 methodology is to evaluate the maximum efficiency limited by thermodynamics. This limit is
96 achieved by defining an ideal (reversible) process. A set of non-idealities in the form of
97 technological limitations are added systematically in series to go from the thermodynamics
98 limited to the technology limited cases. The difference between the thermodynamics limited
99 and technology limited efficiencies can thus be attributed to the different sets of
100 irreversibilities and quantified. This is represented visually in Figure 1.

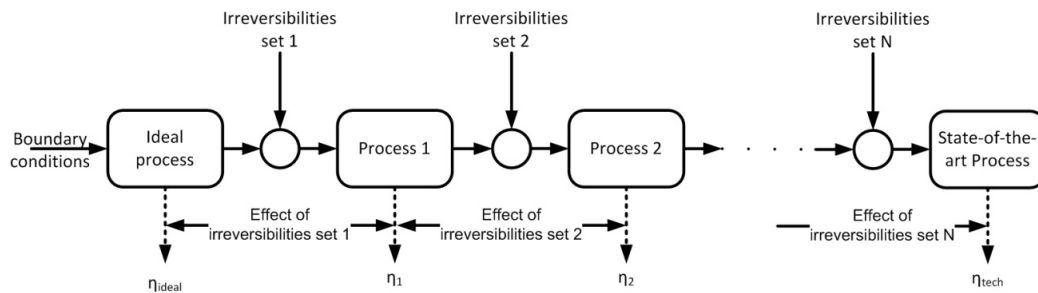


Figure 1. Representation of the systematic methodology for benchmarking

101
102 This methodology is applied to a coal fired power plant to identify and quantify the sources
103 and scope for improvements.

104 3. The reference plant

105 A 754 MWe pulverized coal based power plant has been used as the reference for a
106 benchmarking study [14]. A simplified flowsheet with exergy flow data are shown in Figure 2
107 The fuel is Bituminous Douglas Premium coal, and the air factor is 1.22. The main parameters
108 of the reference plant are presented in Table A1 (Appendix). The coal characteristics and the
109 composition of the atmospheric air are listed in Tables A2 and A3 respectively.

110

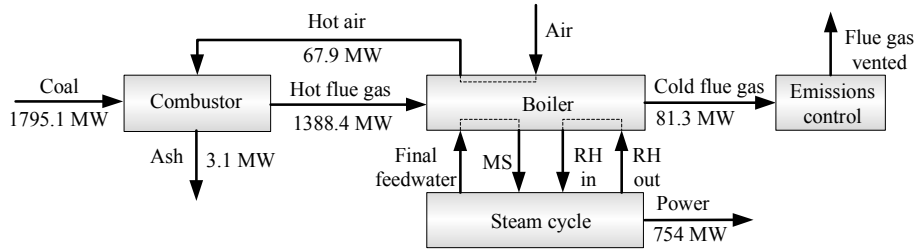


Figure 2 The reference coal based power plant with exergy flows

111

112

113

The procedure for calculating the chemical exergy of substances, the exergy of process

114

streams and the exergy balances for process units are described in the literature[15, 16]. The

115

reference state (marked as “0”) is $T_0=15^\circ\text{C}$, $p_0=1.01$ bar (i.e. 1 atm). The standard chemical

116

exergy of pure substances, e_{ch}^0 [kJ/mole], can be found in Szargut[16] and converted into the

117

corresponding reference state. The chemical exergy of a material stream \dot{E}_{ch} [kW] is

118

calculated using Eq. (1).

119

120

$$\dot{E}_{ch} = \dot{F} \sum_i (x_i e_{ch,i}^0) + \dot{F} \bar{R} T_0 \sum_i (x_i \ln x_i) \quad (1)$$

121

where \dot{F} [mole/s] is the molar flow of the stream and x_i is the molar fraction of component i .

122

The physical (thermo-mechanical) exergy of a stream \dot{E}_{ph} [kW] is equal to the amount of

123

work arising when changing a stream reversibly from process conditions (T, p) to the

124

reference conditions (T_0, p_0), and is calculated by Eq. (2) for the general case of multiple

125

phases.

126

$$\dot{E}_{ph} = \left[\sum_j (\dot{F}_j h_j) - \sum_j (\dot{F}_{0,j} h_{0,j}) \right] - T_0 \left[\sum_j (\dot{F}_j s_j) - \sum_j (\dot{F}_{0,j} s_{0,j}) \right] \quad (2)$$

127

Here, h [kJ/mole] and s [kJ/(mole·K)] are the molar enthalpy and entropy of the stream, and

128

j is the phase index.

129 The total exergy of a stream \dot{E}_{tot} [kW] at process conditions (T, p) is given as:

$$130 \quad \dot{E}_{tot} = \dot{E}_{ch} + \dot{E}_{ph} \quad (3)$$

131 The irreversibility of a unit operation, \dot{I} [kW], can be calculated by:

$$132 \quad \dot{I} = \dot{E}^{in} - \dot{E}^{out} \quad (4)$$

133 where \dot{E}^{in} [kW] and \dot{E}^{out} [kW] are the exergy entering and exiting the unit respectively.

134 The theoretical minimum work required for a unit operation, \dot{W}_{min} [kW], is equal to the
135 difference in exergy between the products and the feeds, and can be calculated by Eq. (5)[15].

$$136 \quad \dot{W}_{min} = \sum_{product} \dot{E}_{tot}^{product} - \sum_{feed} \dot{E}_{tot}^{feed} \quad (5)$$

137 Here, $\dot{E}_{tot}^{product}$ [kW] is the exergy of a product stream and \dot{E}_{tot}^{feed} [kW] is the exergy of a feed
138 stream.

139 According to the methods described by Szargut[16], the chemical exergy of the coal feed
140 (Table A2) is calculated to be 27,295 kJ/kg using Eq. (6).


$$141 \quad e_{ch,coal}^0 = \varphi(\text{LHV})^0 \quad (6)$$

142 Here, $(\text{LHV})^0$ [kJ/kg] is the lower heating value of coal at the reference conditions (T_0, p_0) ,

143 and φ is the ratio of the chemical exergy to the lower heating value, calculated by[16]:

$$144 \quad \varphi = 1.0437 + 0.1896(h/c) + 0.2499(o/c) + 0.0428(n/c) \quad (7)$$

145 where c, h, o and n are the mass fractions of carbon, hydrogen, oxygen and nitrogen in the
146 ultimate analysis of coal (dry basis) respectively.

147 For the reference plant, the exergy of the coal feed is calculated to be 1,795.1 MW and the
148 thermal input (LHV) is 1,655.3 MW. After combustion, the total exergy of the flue gas is
149 1,388.4 MW. The mass fraction of the major components of the ash is: SiO_2 -0.45; Al_2O_3 -0.3;
150 CaO -0.07; Fe_2O_3 -0.03; SO_3 -0.035[5]. The chemical exergy of ash is calculated to be 330
151 kJ/kg, equal to 0.17% of the exergy of the coal feed (3.1 MW), and is thus negligible. The
152 exergy values for main streams are presented in  Fig.

153 **4. Assessments on the thermal efficiency**

155 For the coal feed, the maximum work output is equal to its chemical exergy if the coal to
156 power process is reversible. The chemical exergy of the coal feed is calculated to be 1.08
157 times the lower heating value, while the thermal efficiency of the reference plant is 45.5%.
158 Ideal reversible processes for reaction, separation and heat transfer are presented in the
159 literature[15]. Such processes are infeasible in practice with respect to limitations in
160 technologies, investment cost and plant lifetime. Proper driving forces are necessary and thus
161 causing irreversibilities. The oxidation (combustion) of coal, the heat transfer between the
162 flue gas and the working fluid of the power cycle, and the power cycle itself are the major
163 sources of irreversibilities. The following sections illustrate how the thermal efficiency is
164 reduced from its theoretical maximum to practical values by thermodynamic, technical and
165 economic factors.

166 **4.1. Combustion losses**

168 The chemical energy of coal is released when the coal is oxidized to CO_2 and H_2O . Direct
169 combustion with air is the most common way for the oxidation of coal. In the case of
170 complete stoichiometric combustion, the adiabatic flame temperature is calculated to be 2,332
171 K. The exergy destruction related to stoichiometric combustion is determined to be 30.4% of

172 the exergy of the coal. The chemical exergy of the flue gas, which corresponds to 3.5% of the
173 exergy of the coal feed, has not yet been recovered by current technologies (unless the flue
174 gas is further utilized as feed for other processes instead of being vented), meaning that the
175 theoretical work that can be recovered from the flue gas is 66.1% of the exergy of the coal
176 feed. The maximum thermal efficiency that can be obtained is thus 71.4% (determined as the
177 ratio between the theoretical work that can be recovered from the flue gas (physical exergy)
178 and the thermal input).

179 At temperatures higher than 1,250 K, components such as CO₂ and H₂O will dissociate[17].
180 The equilibrium temperature (the temperature when chemical equilibrium is achieved) is
181 obtained as 2,229 K, around 100 K lower than the adiabatic flame temperature of complete
182 combustion. The exergy destruction is the same as for the complete combustion case.
183 However, the chemical exergy of unburned CO and H₂ in the flue gas is not expected to be
184 recovered when the flue gas is cooled since the chemical equilibrium can not be achieved in
185 finite time.

186 4.1.1. Thermodynamic analysis of the combustion processes 187

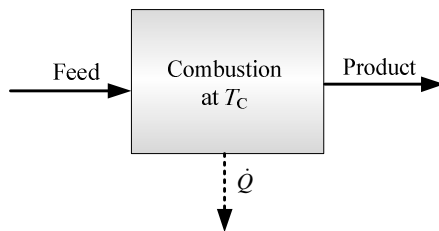


Figure 3 An isothermal combustion process

188 For an isothermal combustion process as shown in Figure 3, the entropy balance and energy
189 balance can be written as:
190

$$191 \dot{S}_{\text{generation}} = \dot{S}_{\text{product}} - \dot{S}_{\text{feed}} + \dot{Q}/T_C = \Delta\dot{S} + \dot{Q}/T_C \quad (8)$$

192

193
$$\dot{Q} = \dot{H}_{\text{feed}} - \dot{H}_{\text{product}} = -\Delta\dot{H} \quad (9)$$

194

195 where $\dot{S}_{\text{generation}}$ is the entropy generation caused by combustion irreversibilities, \dot{S}_{product} and
196 \dot{S}_{feed} are the entropy of the product and the feed, $\Delta\dot{S}$ is the entropy difference between the
197 product and the feed, \dot{Q} is the heat removed from the system, T_C is the operating temperature,
198 \dot{H}_{feed} and \dot{H}_{product} are the enthalpies of the feed and the product, and $\Delta\dot{H}$ is the enthalpy
199 difference between the product and the feed.

200 If the process is reversible, $\dot{S}_{\text{generation}} = 0$, then $T_C = \Delta\dot{H} / \Delta\dot{S}$. This temperature is defined as
201 the combustion temperature[18]. The change in Gibbs free energy $\Delta\dot{G}$ is zero at T_C [19]. This
202 temperature (T_C) can be understood as the one where the combustion reaction can take place
203 reversibly, i.e. the (practically impossible) condition is necessary to be maintained for the
204 entire combustion process. The changes in the enthalpy and entropy differences between the
205 product and the feed with the temperature are negligible[3, 18, 19], thus $T_C \approx \Delta\dot{H}_0 / \Delta\dot{S}_0$,
206 where $\Delta\dot{H}_0$ and $\Delta\dot{S}_0$ are the enthalpy and entropy differences between the product and the
207 feed for a reaction at ambient temperature T_0 . The combustion temperature of bituminous
208 coal can be as high as 27,466 K[3], which is much higher than the stoichiometric adiabatic
209 combustion temperature (2,332 K). In addition, the isothermal condition is impossible to
210 maintain in practice. Irreversibilities will also be introduced when the reactants are heated
211 from ambient temperature to the combustion temperature and the products are cooled from
212 combustion temperature to ambient temperature. Thus the irreversibilities for the combustion
213 process (air is used as oxidant) are considerable.

214 In the case of adiabatic combustion of H_2 and CH_4 , the irreversibilities are mainly caused by:
215 (1) combined diffusion/fuel oxidation, (2) internal thermal energy exchange, and (3) the
216 product mixing process[20]. The internal thermal energy exchange is responsible for more
217 than 2/3 of the total losses. Similar results have also been observed for the combustion of
218 carbon[21], i.e. internal thermal energy exchange and the chemical reaction (fuel oxidation)
219 are responsible for the major losses.

220 221 **4.1.2. Reducing combustion irreversibilities**

222 The following options are available to reduce the combustion irreversibilities:

223 (1) *Converting coal into syngas by gasification (CO and H_2)*. The gasification process has
224 lower exergy destruction than the combustion process[21]. The syngas is further converted
225 into H_2 that can be oxidized in fuel cells. The fuel cells can achieve a high thermal
226 efficiency at a much lower temperature compared to heat engines[19]. However, current
227 gasification processes are not competitive to direct combustion with respect to economic
228 considerations. Large scale implementation of fuel cells is also indeed a technical
229 challenge.

230 (2) *Shifting direct combustion processes to chemical looping combustion (CLC)*. Metal
231 oxides can be used as the oxidant. The combustion temperature T_c of CLC processes can be
232 reduced to feasible levels (e.g. lower than 1,000 K)[3], thus the irreversibilities related to
233 the reaction are reduced. The irreversibilities caused by internal thermal energy exchange
234 and product mixing can also be reduced. Further technology developments are required to
235 implement the CLC technology and much research is ongoing[22].

236 (3) *Increasing the operating temperature (adiabatic temperature)*. The exergy destruction
237 related to combustion is lower at higher operating temperatures. Theoretically, very high

238 operating temperatures can be achieved by preheating the air feed. However, the
239 temperature is limited by materials of construction. In addition, the dissociation of CO₂ and
240 H₂O increases at high temperature. The CO and H₂ can not be completely oxidized into
241 CO₂ and H₂O when the flue gas is cooling down due to limited time for heat exchange.

242 (4) *Reducing the exergy destruction related to internal thermal energy exchange.* The
243 preheating of air can reduce such losses.

244 (5) *Reducing the exergy destruction related to product mixing.* Such losses are small, but can
245 still be reduced by reducing the air factor (defined as the ratio of the actual air feed to the
246 stoichiometric air feed) or using pure O₂ or metal oxides. Lower air factors, however, can
247 result in incomplete combustion of coal.

248 The possible change in the irreversibilities of other units should also be taken into
249 consideration when the combustion irreversibilities are reduced. For the reference power
250 plant, the following three practical measures are investigated: (i) preheating the air (referred
251 to items (3) and (4) above), (ii) reducing the air factor (referred to items (4) and (5) above)
252 and (iii) using pure O₂ (referred to items (3), (4) and (5) above).

253 Figure 4 shows the exergy destruction of the combustion process (as percentage of the exergy
254 of the coal feed) and the adiabatic flame temperature at different air feed temperatures and air
255 factors (referred to the numbers for each curve in the figure). The results are obtained using
256 two models: (1) complete combustion and (2) chemical equilibrium. The exergy destruction is
257 almost the same for the two combustion models. This is explained by relatively low T_C for
258 CO and H₂ (3,276.5 K and 5,454 K respectively according to literature[3]). The adiabatic
259 flame temperature is not far away from T_C , thus the exergy destruction is very small if the
260 unburned CO and H₂ (determined by the equilibrium model) are burned completely.

261 However, the chemical exergy of the unburned CO and H₂ may be lost in the stack if the CO
 262 and H₂ have not been oxidized when the flue gas is cooled.

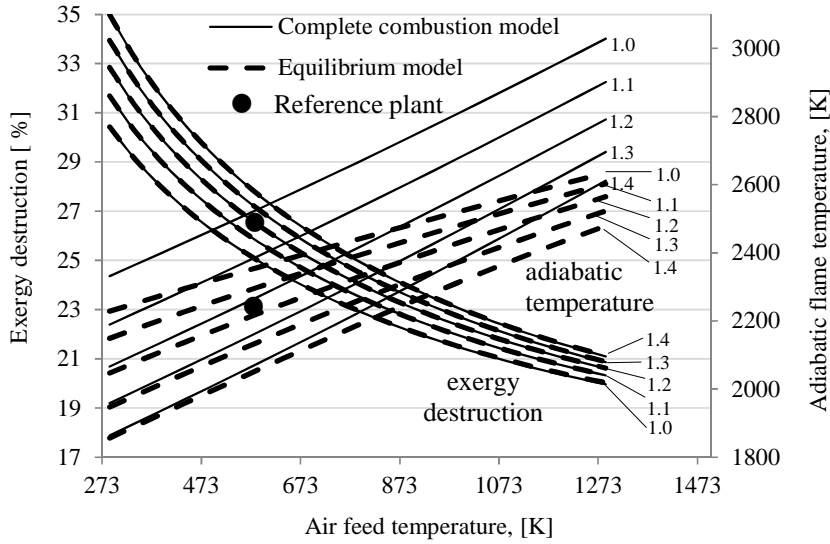


Figure 4 Exergy destruction due to combustion [% of the exergy of the coal]

263
 264 Preheating of air can reduce the losses caused by internal thermal energy exchange and
 265 combustion reactions. The exergy destruction is reduced from 30.4% to 20.0% when the air is
 266 preheated from 288 K to 1,288 K in the case of stoichiometric combustion. Without any
 267 preheating of air, the exergy destruction increases from 30.4% to 35.0% when the air factor
 268 increases from 1.0 to 1.4. The excess air reduces the adiabatic flame temperature, thus
 269 increases the exergy destruction caused by combustion reactions. The exergy destruction
 270 related to mixing and the internal thermal energy exchange also increases. When the air is
 271 preheated, the influence of the air factor on the exergy destruction is reduced. When the air
 272 factor is 1.22 (the reference plant) in the case of no preheating, the exergy of the combustion
 273 product is 67.0% of the exergy of the coal feed, where the physical exergy and the chemical
 274 exergy contribute 63.0% and 4.0% respectively.

275 When pure O₂ is used for combustion (oxy-combustion), the exergy destruction related to the
276 combustion reaction, mixing (N₂ is not present) and internal thermal energy exchange (no
277 heating of N₂) is reduced. In case of stoichiometric combustion without preheating of air, the
278 exergy destruction for the combustion process is calculated to be 20.5% of the coal feed.
279 However, the extremely high adiabatic flame temperature (5,495 K) requires dilution. In
280 addition, the production of pure O₂ introduces air separation units and thus new losses. When
281 CO₂ capture is included, however, oxy-combustion is a promising alternative[23].

282 **4.2. Low temperature heat losses**

283 In the reference power plant, the exhaust flue gas temperature is 393 K. The physical exergy
284 of the flue gas is calculated to be 0.96% of the thermal input. The reduction in low
285 temperature heat wasted or recovery of this heat is an important way to improve the thermal
286 efficiency. The low temperature heat losses can also be reduced by decreasing the air factor
287 and the flue gas temperature. Organic Rankine Cycles (ORCs) and some other cycles have
288 been proposed for recovering low temperature heat[24]. This topic is, however, not discussed
289 in detail in this paper.

290 The influence of the air factor (denoted by f) on low temperature heat losses can be explained
291 using Figure 5. The energy balance is assumed to be satisfied for the case of stoichiometric
292 combustion ($f=1$), and is represented by the streams in solid lines. Note that the heat losses
293 related to surface radiation and convection and the steam losses due to boiler blowdown and
294 surface blowoff for impurity removal, and any other steam losses are neglected. The heat loss
295 caused by the ash is also neglected. If the air factor increases from 1 to f , more coal (\dot{m}'_{coal}) is
296 burned in order to heat the additional flue gas (\dot{m}'_{FG}) from ambient temperature to the flue
297 gas temperature. The dashed lines show the combustion of the additional coal. Note that the
298 flue gas represented by dashed lines includes the products of the combustion of the additional

299 coal and the excess air. The mass balance should be satisfied for the dashed streams, as shown
300 by Eq. (10).

$$301 \quad \dot{m}'_{\text{coal}} + \dot{m}'_{\text{air}} = \dot{m}'_{\text{FG}} + \dot{m}'_{\text{ash}} \quad (10)$$

302 Here \dot{m}'_{air} is the mass flow of the additional air to be used, $\dot{m}'_{\text{air}} = f\omega\dot{m}'_{\text{coal}} + (f-1)\omega\dot{m}'_{\text{coal}}$,
303 where ω is the stoichiometric ratio ($\omega = 8.8122$ for the coal feed). \dot{m}'_{ash} is the mass flow of
304 the additional ash produced, thus $\dot{m}'_{\text{ash}} = 0.1415\dot{m}'_{\text{coal}}$ (according to Table A2). Eq. (10) can
305 be rearranged as:

$$306 \quad \dot{m}'_{\text{FG}} = (0.8585 + 8.8122f)\dot{m}'_{\text{coal}} + 8.8122(f-1)\dot{m}'_{\text{coal}} \quad (11)$$

307 According to the definition of the lower heating value (LHV), the following energy balance
308 can be obtained:

$$309 \quad \dot{m}'_{\text{coal}}(\text{LHV}) = \dot{m}'_{\text{FG}}(h'_{\text{FG},T_{\text{FG}}} - h'_{\text{FG},T_0}) \quad (12)$$

310 where $h'_{\text{FG},T_{\text{FG}}}$ and h'_{FG,T_0} are the specific enthalpies of the additional flue gas at exhaust
311 temperature (T_{FG}) and ambient temperature (T_0).

312

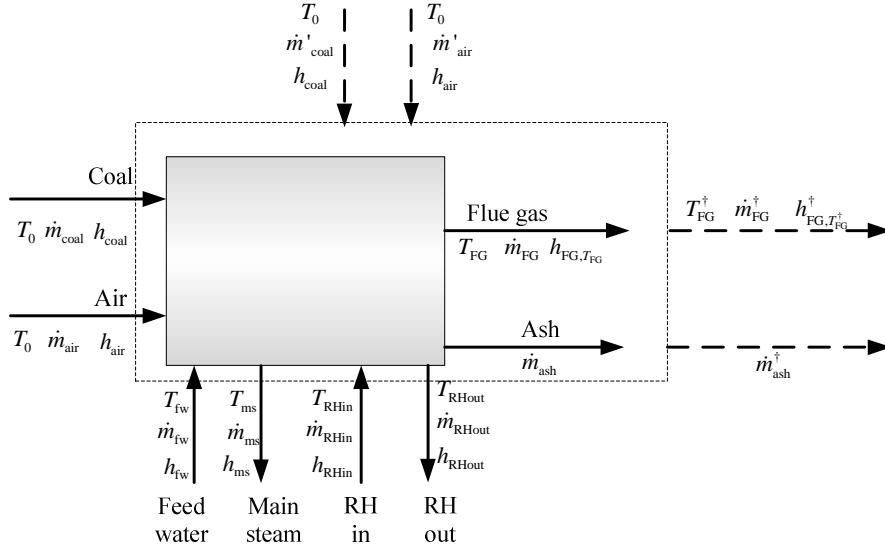


Figure 5 Mass and energy balances for investigating the influence of the air factor (f)

313

314 For a given T_{FG} , the influence of the air factor on the thermal efficiency can be investigated

315 based on Eqs. (11) and (12). Similarly, the influence of the exhaust flue gas temperature on

316 the thermal efficiency can also be investigated. Figure 6 shows the mass and energy balances

317 when the flue gas temperature changes from T_{FG} (the box in solid lines) to T_{FG}^\dagger (the box in

318 dashed lines). Note that the flue gas represented by the dashed lines includes the gas products

319 resulting from the burning of the two portions of coal feed (\dot{m}_{coal} and \dot{m}'_{coal}). More (or less)

320 coal is consumed when the flue gas temperature increases (or decreases) in order to maintain

321 the energy balance. The following energy balance can easily be obtained from Figure 6.

$$322 \quad LHV(\dot{m}'_{coal}) = \dot{m}_{FG}^\dagger (h_{FG, T_{FG}^\dagger}^\dagger - h_{FG, T_0}) - \dot{m}_{FG} (h_{FG, T_{FG}} - h_{FG, T_0}) \quad (13)$$

323 where $h_{FG, T_{FG}}$ and h_{FG, T_0} are the specific enthalpies of the flue gas at exhaust temperature (T_{FG})

324 and ambient temperature (T_0). For a given f , the influence of the flue gas temperature on the

325 thermal efficiency can then be determined.

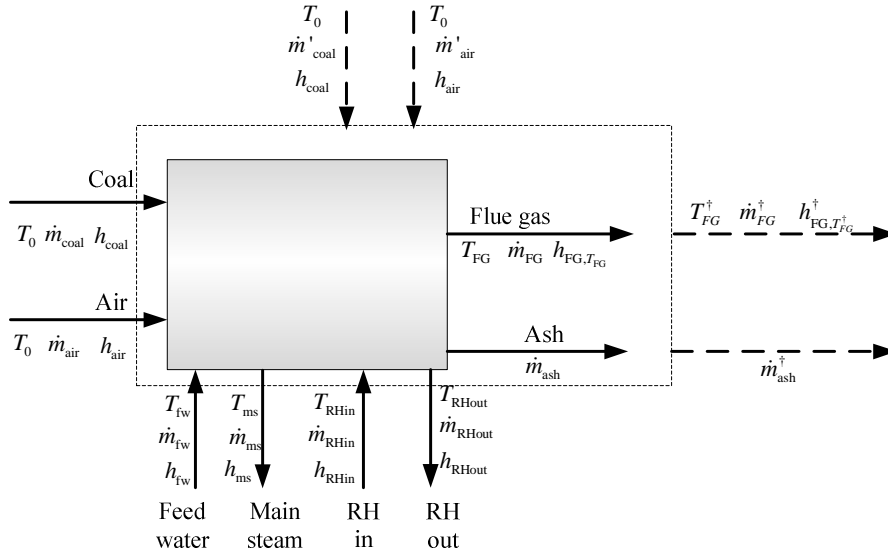


Figure 6 Mass and energy balances for investigating the influence of the flue gas temperature

326
327

328 The results are illustrated in Figure 7. When the flue gas temperature is 393 K (the reference
 329 plant), the thermal efficiency increases from 45.2% to 45.9% when the air factor is reduced
 330 from 1.4 to 1.0. The thermal efficiency increases by 0.1% points on average when the air
 331 factor is reduced by 0.057. When the air factor is 1.22 (the reference plant), the thermal
 332 efficiency increases from 45.5% to 46.6% if the flue gas temperature decreases from 393 K to
 333 345 K. Such reduction in flue gas temperature can be achieved by using flue gas as heat
 334 source in air preheaters that can withstand the acid corrosion[5]. The spread and distribution
 335 of the flue gas from the stack limits the flue gas temperature to 345 K[5]. If the flue gas could
 336 be further cooled to 308 K (this temperature is limited by the temperature driving forces of
 337 heat exchangers), the thermal efficiency would increase to 47.4%. It is found that for every
 338 reduction of 4.5 K in flue gas temperature, the thermal efficiency increases by ~0.1% points.
 339 The air factor has negligible influence on the thermal efficiency when the flue gas is cooled to
 340 ambient temperature. This is reasonable since the heat losses are very small when the flue gas
 341 exits at around ambient temperatures.

342 It should be noted that the thermal efficiency increases by around 2% points (according to
343 Figure 7) when the low temperature heat is completely recovered in the boiler system, but by
344 a maximum of 0.96% points (corresponding to the physical exergy of the flue gas) if the low
345 temperature heat is converted into work by additional ORCs. This difference is explained by
346 the very low quality (exergy) of the low temperature heat and thus the very low efficiency of
347 ORCs. When the low temperature heat is recuperated in the boiler system, less coal is burnt
348 and thus the irreversibilities are reduced. The capital cost is also a considerable challenge for
349 implementing ORCs. Thus, it is reasonable to put efforts into reducing low temperature heat
350 losses from the boiler system before using ORCs to recover work from the low temperature
351 heat. This can be implemented simply by increasing the size of the air preheater (reducing the
352 temperature difference at the pinch point of the air preheater), resulting in more low
353 temperature heat being recirculated into the burner.

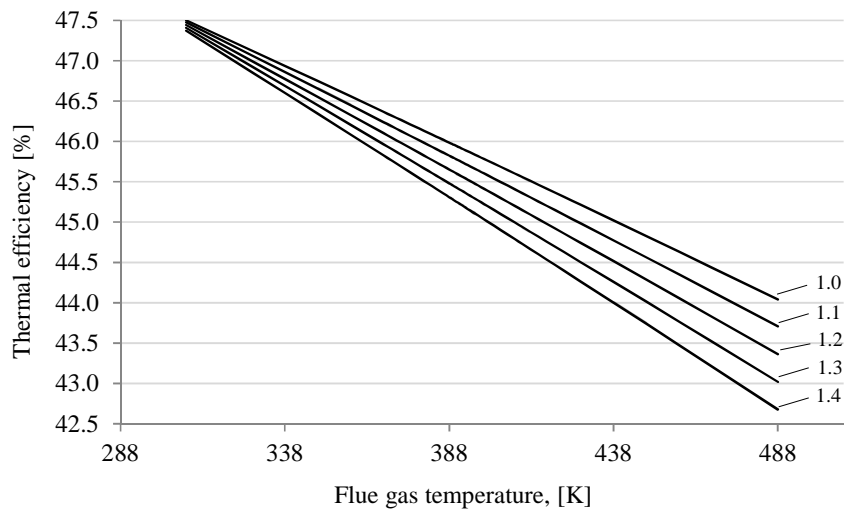


Figure 7 Influence of the air factor and flue gas temperature on thermal efficiency

354
355

356 4.3. Heat transfer between the flue gas and the working fluid

357 Combustion heat is normally converted into work by heat engines. The efficiency of heat
358 engines is limited by the Carnot efficiency. An ideal working fluid receives heat from the flue

359 gas with small temperature differences and rejects it to the ambient environment (normally to
 360 cooling water). Such a process is illustrated in Figure 8(a) and explained as following: the
 361 fluid is reversibly heated by the flue gas (2-3) after being isentropically compressed (1-2), and
 362 then reversibly cooled (4-1) at ambient temperature after being isentropically expanded (3-4).
 363 In the case of reversible heat transfer, the maximum work output is equal to the changes in
 364 exergy for the flue gas between the adiabatic flame temperature (T_{ad}) and the exhaust
 365 temperature (T_{FG}) for the reference plant, the physical exergy of the flue gas is 63.0% of the
 366 exergy of the coal, thus the maximum thermal efficiency (referred to LHV) is 68.3%.

367

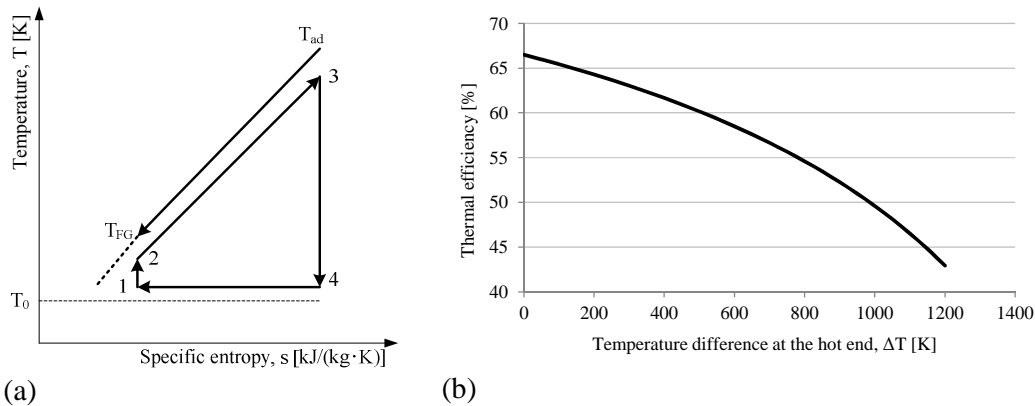


Figure 8 Ideal heat engine: (a) T-s diagram, (b) Thermal efficiency

368

369

370

If the heat capacities of the flue gas and the working fluid are assumed to be constant, and

371

assuming $T_2 = T_1 = T_0$ and $T_{FG} = 308.15$ K, the plant thermal efficiency is determined by the

372

temperature difference in the hot end ($\Delta T = T_{ad} - T_3$). Figure 8(b) illustrates the influence of

373

ΔT on the thermal efficiency. The thermal efficiency decreases from 66.5% to 44.8% when

374

ΔT increases from 0 K to 1,150 K. For $\Delta T = 1150$ K, T_3 is equal to 878.6 K. This is very

375

close to the main steam temperature (873 K) in the reference plant, the thermal efficiency of

376

which is 45.5%. When T_3 is 1,073 K (800°C, corresponding to ultra-supercritical steam

377

cycles), the thermal efficiency is 51.0%.

378 In order to reduce the exergy destruction caused by heat transfer, it is useful to explore an
379 ideal working fluid for the cycle “1-2-3-4-1”. Such working fluids are, however, not available.
380 One alternative is to use a mixture of components as the working fluid (e.g. the Kalina
381 cycle[25]). The boiling points are not constant in Kalina cycles, thus the exergy destruction
382 related to heat transfer can be reduced. Another alternative is to use a combination of several
383 cycles: liquid metal such as potassium and mercury is used for the high temperature range[4];
384 water is used for the medium temperature range; organic substances or CO₂ are used for the
385 low temperature range. Gas turbine combined cycles are more commonly used, where the
386 air/exhaust flue gas is used as working fluid for the higher temperature range, and water is
387 used for the lower temperature range.

388 389 **4.4. Thermal efficiency improvement for the steam cycle**

390 Steam Rankine cycles are most commonly used in coal based power plants. The heat transfer
391 between the flue gas and the steam causes considerable exergy destructions due to large
392 temperature differences. Other irreversibilities are caused by the inefficiencies of steam
393 turbines, pumps, and the heat transfer with finite temperature differences in the regenerative
394 feedwater preheaters and the condenser.

395 The maximum temperature and pressure of the steam are mainly limited by the construction
396 materials of steam generators and steam turbines[5]. The steam temperature is expected to
397 reach 973 K (700°C) in the near term and 1,073 K (800°C) in the long term. With reference to
398 Figure 5, the heat supplied to the steam cycle, \dot{Q}_{SC} , is calculated by:

$$399 \quad \dot{Q}_{SC} = \dot{m}_{ms} h_{ms} + \dot{m}_{RHout} h_{RHout} - \dot{m}_{fw} h_{fw} - \dot{m}_{RHin} h_{RHin} \quad (14)$$

400

401 where \dot{m}_{fw} , \dot{m}_{ms} , \dot{m}_{RHin} and \dot{m}_{RHout} are the mass flows of boiler feedwater, main steam, cold
 402 reheating steam and hot reheating steam; h_{fw} , h_{ms} , h_{RHin} and h_{RHout} are the corresponding
 403 specific enthalpies of the streams. According to the data presented in Table A1 for the
 404 reference plant and steam properties, \dot{Q}_{SC} is calculated to be 1,567.6 MW. The boiler
 405 efficiency (the ratio of \dot{Q}_{SC} to the thermal input of the coal feed) is thus 94.7%.

406 The maximum work that can be produced from the steam cycle, \dot{W}_{SC} , is calculated by:

$$407 \quad \dot{W}_{SC} = \dot{m}_{ms}e_{ms} + \dot{m}_{RHout}e_{RHout} - \dot{m}_{fw}e_{fw} - \dot{m}_{RHin}e_{RHin} \quad (15)$$

408
 409 where e_{fw} , e_{ms} , e_{RHin} and e_{RHout} are the specific exergies of boiler feedwater, main steam, cold
 410 reheating steam and hot reheating steam. \dot{W}_{SC} is calculated to be 916.9 MW for the reference
 411 plant. Thus, the theoretical maximum thermal efficiency of the steam cycle (cycle efficiency)
 412 for the given parameter values for feedwater and steam is 58.5%. The maximum thermal
 413 efficiency of the entire plant is then calculated to be 55.4% (by including the boiler
 414 efficiency). This value is higher than the value (44.8%) predicted in Figure 8(b), since the
 415 boiler feedwater and the reheating steam are fed at temperatures much higher than ambient,
 416 while the boiler feedwater is fed at ambient temperature for the case shown in Figure 8.

417 **4.4.1. Influence of main steam parameters on thermal efficiency**

418 By considering Eq. (14), and assuming that reheating is not applied, the mass flow of the main
 419 steam is determined by the parameters (temperature and pressure) of the boiler feedwater and
 420 the main steam. The maximum work output from the steam cycle is calculated by Eq. (15).
 421 Thus, the maximum thermal efficiency of the entire plant can be calculated. The influence of
 422 the main steam parameters on the thermal efficiency is shown in Figure 9. Two feedwater
 423 temperatures are investigated: 308 K (corresponding to the outlet temperature of the

424 condenser in the reference plant; represented by the dashed lines) and 581 K (corresponding
 425 to the final feedwater temperature, FFWT, in the reference plant; represented by the solid
 426 lines). Since the benchmarking methodology in this paper is to evaluate the thermal efficiency
 427 by stepwise investigation from theoretical to practical values, the condensate from the
 428 condenser is assumed to be reversibly brought to final feedwater conditions. The work
 429 calculated by the exergy difference between the final feedwater and the condensate is
 430 included in the calculation of thermal efficiency. The pressure losses are neglected.

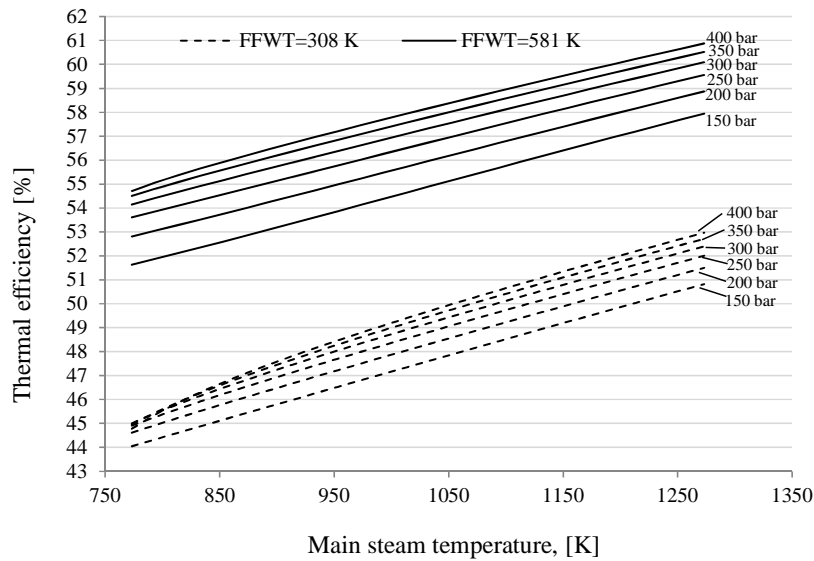


Figure 9 Influence of the main steam parameters on the thermal efficiency

431
 432

433 The results in Figure 9 clearly illustrate the benefit from feedwater preheating that is today
 434 commonly applied in steam power plants. It can also be noticed that the effect of pressure is
 435 that the thermal efficiency decreases with increasing pressure. This can be explained by the
 436 smaller changes in specific entropy with pressure at higher pressures. Eq. (16) shows how
 437 specific entropies of the main steam and boiler feedwater (s_{ms} and s_{fw}) affect the physical
 438 (thermo-mechanical) exergy. The heat transferred to the steam cycle is fixed,

439 $\dot{Q}_{SC} = \dot{m}_{ms}(h_{ms} - h_{fw})$, thus the exergy transferred to the steam cycle, \dot{E}_{SC} , is mainly
440 influenced by the entropy differences of the main steam and the feedwater.

$$441 \quad \dot{E}_{SC} = \dot{m}_{ms}e_{ms} - \dot{m}_{fw}e_{fw} = \dot{m}_{ms}[(h_{ms} - h_{fw}) - T_0(s_{ms} - s_{fw})] \quad (16)$$

442

443 When the feedwater temperature is 308 K (dashed lines in Figure 9) and the steam
444 temperature is about 773 K, the steam pressure has negligible influence on the thermal
445 efficiency in the case that the pressure exceeds 300 bar. The thermal efficiency increases
446 almost linearly with temperature when the feedwater temperature is 581 K (solid lines in
447 Figure 9). It increases from 54.1% to 60.0% when the steam temperature increases from 773
448 K to 1,273 K for a pressure of 300 bar. An average increase of 0.1% points in thermal
449 efficiency is obtained for every increment of 8 K in the steam temperature. The thermal
450 efficiency increases from 52.8% to 56.2% when the pressure increases from 150 bar to 400
451 bar for a steam temperature of 873 K. The thermal efficiency increases by approximately
452 0.1% points for every increment of 10 bar in the pressure range of 250-350 bar.

453 The thermal efficiency is 56.6-57.1% in the pressure range of 300-350 bar when the steam
454 temperature is 973 K. This is the common target in the very near future based on the
455 development of nickel-based alloys[24]. If the steam temperature reaches around 1,073 K, the
456 thermal efficiency is 57.8-58.2% for the same pressure range. The thermal efficiency
457 achievable is 60.9% at 400 bar and a steam temperature of 1,273 K (the very long-term
458 target). However, the thermal efficiency presented in Figure 9 is the *theoretical* maximum
459 efficiency without reheating. In practice the steam from the last stages of the low pressure
460 (LP) turbine should neither be too wet nor too hot. Thus the temperature and pressure of the
461 main steam should be matched with each other.

462 **4.4.2. Final feedwater temperature**

463 Figure 9 shows the established fact that the feedwater temperature has a significant influence
464 on the thermal efficiency. Higher feedwater temperature increases the mean temperature of
465 heat addition from the flue gas to the steam cycle. Thermal efficiency of Rankine cycles
466 increases when the average temperature of heat addition is higher. However, when the amount
467 of heat from the flue gas and the main steam temperature are fixed, the mass flow of the
468 feedwater and thus the size and capital cost of equipment increases. High feedwater
469 temperature is normally achieved by regenerative pre-heating. The final feedwater
470 temperature (FFWT) should be optimized with respect to the thermal efficiency and
471 investment cost. For subcritical cycles, the maximum FFWT is the boiling point of the main
472 steam. The maximum thermal efficiency is obtained by optimizing the heat loads of each
473 feedwater. An infinite number of heaters is required to achieve the maximum thermal
474 efficiency when the feedwater is supplied at the boiling point[26]. For supercritical and ultra-
475 supercritical cycles, there is no transition between vapor and liquid. The maximum feasible
476 FFWT is limited by the pinch temperature differences of the economizer and the air preheater,
477 as illustrated in Figure 10. When the temperatures in the cold end of the preheater (the air
478 inlet temperature $T_{air,c}$ and the flue gas exhaust temperature T_{FG}) are fixed, the FFWT is
479 limited by the pinch temperature differences of the economizer (ΔT_{eco}) and the preheater (
480 ΔT_{pre}).

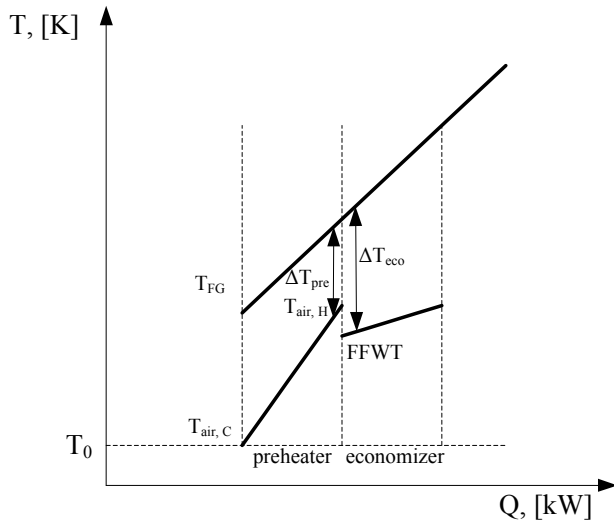


Figure 10 Pinch temperatures of the preheater and economizer

481

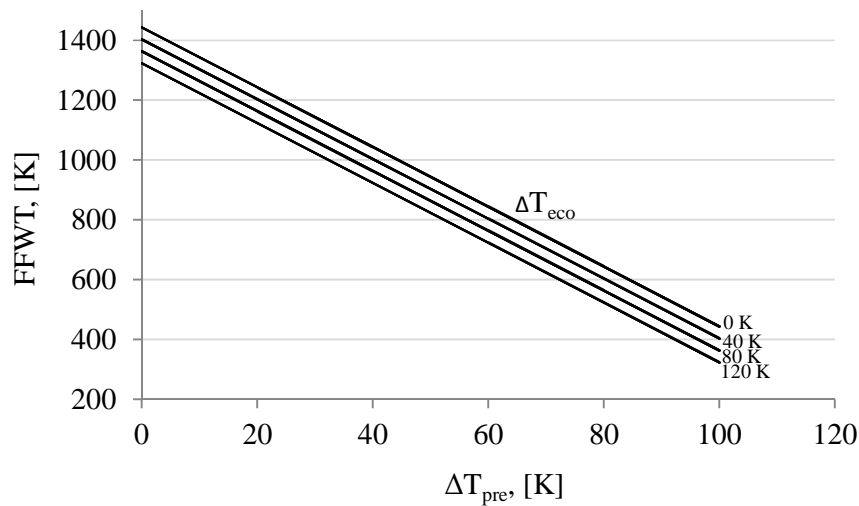


Figure 11 Influence of pinch temperatures for the preheater and economizer on the FFWT

482
483

484 For the reference plant, $T_{FG}=393$ K, $T_{air,c}=288$ K and $f=1.22$. The influence of ΔT_{eco} and
 485 ΔT_{pre} on the FFWT can then be investigated when assuming constant specific heat capacities
 486 of the air and the flue gas, as illustrated in Figure 11. The maximum FFWT is 1,443 K when
 487 both ΔT_{eco} and ΔT_{pre} are 0 K. This temperature is far beyond the maximum temperature of
 488 the superheated steam limited by materials of construction. When ΔT_{eco} and ΔT_{pre} are fixed, a

489 higher FFWT will increase the flue gas exhaust temperature (T_{FG}), thus the low temperature
490 heat losses will increase.

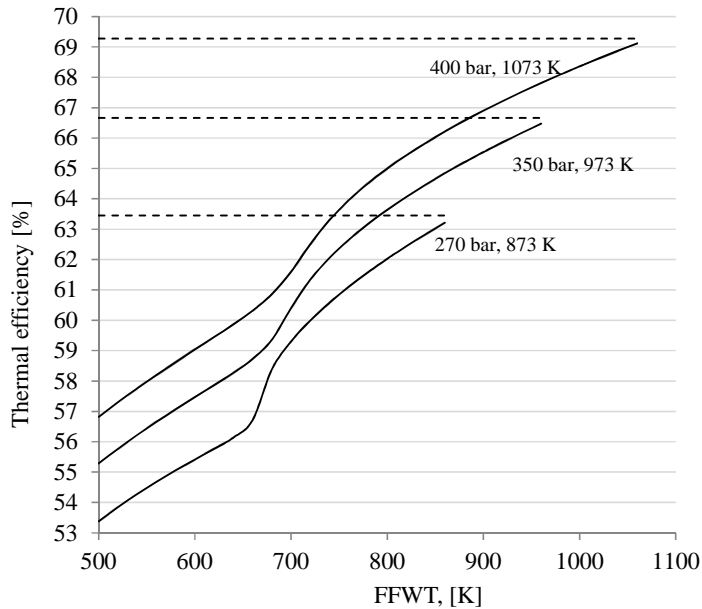


Figure 12 Influence of FFWT on the thermal efficiency

491
492 Similar to the investigation on the influences of steam main parameters presented in Section
493 4.4.1, the maximum work output is calculated by Eq. (15), and the energy consumption for
494 the feedwater heating process is calculated by the exergy differences between the final
495 feedwater and the condensate. The net work production and thus thermal efficiency can then
496 be determined when the FFWT and steam parameters are known. Figure 12 shows the
497 influence of the FFWT on the thermal efficiency of the entire plant for typical main steam
498 parameters (without reheating). The dashed lines just above each curve represent the Carnot
499 efficiency (the mass flow of the main steam is infinitely large). When the FFWT gets close to
500 the main steam temperature, the thermal efficiency is close to the Carnot efficiency. However,
501 the high FFWT increases the mass flow of boiler feedwater and also the number of feedwater
502 heaters. The capital cost thus considerably increases. The improvement is economics limited.

503 The FFWT is typically around 500-600 K[27]. For this range, the thermal efficiency increases
504 almost linearly by 0.1% points for an average increment of 5 K in FFWT. Beyond this range
505 (FFWT>600K), evaporation may take place, thus the curves are non-linear.

506
507 **4.4.3. Reheating and turbine efficiency**

508

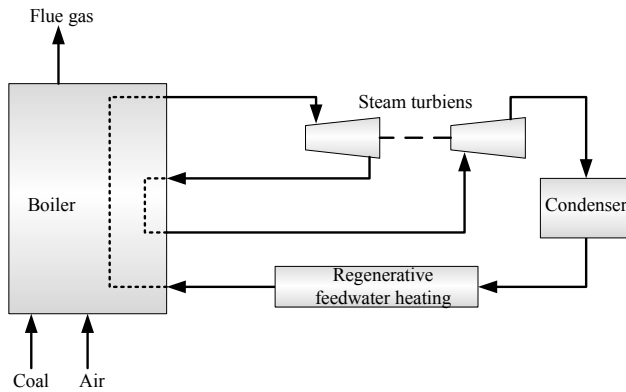


Figure 13 A steam Rankine cycle with reheating

509
510 The main steam can be reheated against the flue gas in the boiler area before it is expanded to
511 the condenser pressure, as illustrated in Figure 13. Reheating is applied in steam cycles for
512 two reasons: (i) reducing the moisture content in the last stages of the turbine and (ii)
513 increasing the mean temperature of heat addition. Reheating with more than two stages has
514 been less discussed in literature since the additional investment cost and the complexity are
515 not expected to be justified by the gain in thermal efficiency. Without considering the
516 investment cost, an infinite number of reheating stages can be imagined. Then the reheating
517 process is an isothermal expansion process, as illustrated by process 2-3 in Figure 14(a). The
518 boiler feedwater (BFW; 1) is heated to the main steam condition (2). The steam is expanded
519 to state 3 at constant maximum temperature. Point 3 has the same entropy as the saturated
520 vapor at the condenser pressure (4; 0.048 bar). The process 3-4 is an isentropic expansion
521 process. The steam is then condensed (4-5), pumped and heated to the feedwater conditions

522 (5-1). The process 5-1 is assumed to be reversible, thus the work consumed in this process is
 523 calculated by the exergy difference of the two states. No steam is extracted for regenerative
 524 preheating. The cycle efficiency is calculated by Eq. (17).

$$525 \quad \eta = (\dot{W}_{23} + \dot{W}_{34} - \dot{W}_{51}) / (\dot{Q}_{12} + \dot{Q}_{23}) \quad (17)$$

526 where \dot{W} and \dot{Q} are the work and heat for the processes.

527 For the reference power plant, the influence of the outlet pressure from the isothermal
 528 expansion (p_3) on the cycle efficiency is shown in Figure 14(b). If no reheating is applied,
 529 $p_3 = p_2 = 270$ bar, the cycle efficiency is 53.4%. In this case, the steam quality is 0.736 at the
 530 outlet of the last stage of the turbine. The thermal efficiency is calculated to be 50.5% by
 531 including the boiler efficiency previously calculated to be 94.7%. Note that if the
 532 condensation process is reversible (all of the condensation heat can be recovered as equivalent
 533 work), the cycle efficiency is calculated to be 58.2%. The corresponding thermal efficiency is
 534 55.1% (by including a boiler efficiency of 94.7%), which is the same as the value obtained in
 535 Figure 12 (FFWT = 581 K). Thus the irreversible condensation process has reduced the
 536 thermal efficiency by 4.6% points (0.551-0.505).

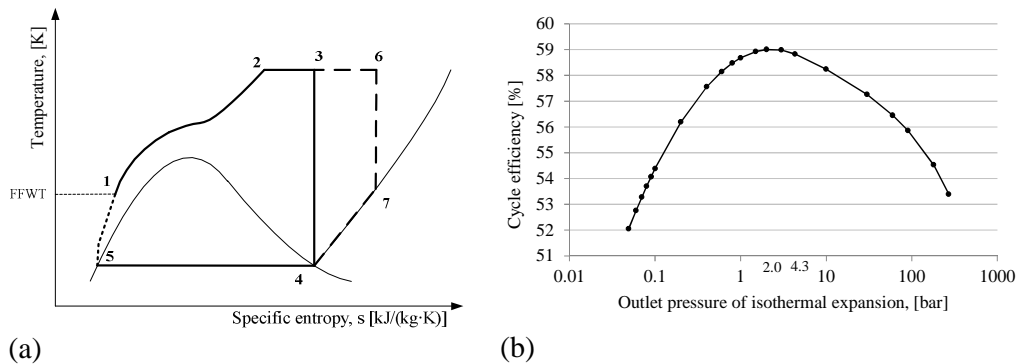


Figure 14 Isothermal expansion: (a) T-s diagram, (b) Cycle efficiency

537 If the main steam is isothermally expanded to 4.3 bar and then isentropically expanded to
 538 0.048 bar, the steam at the outlet of the last stage of the turbine is saturated. The cycle
 539

540 efficiency is 58.8%. However, this is not the maximum efficiency that can be achieved.
541 Instead the main steam can be isothermally expanded to p_6 , and then isentropically expanded
542 to p_7 . In this case, superheated steam (7) is condensed in the condenser. Such a process is
543 shown by dashed lines in Figure 14(a). This process increases the temperature of heat
544 dissipation but also increases the temperature of heat addition. An optimal p_6 can be obtained
545 by iteration when the cycle efficiency is equal to the efficiency of a Carnot cycle operating
546 between the two temperatures T_6 and T_7 , i.e. $(1 - T_7 / T_6)$. For the given process conditions,
547 the optimal pressure is 2.0 bar and the corresponding cycle efficiency is 59.0%. The
548 temperature of the steam from the last turbine stage is 371 K. The observation is useful for the
549 optimization of the reheating pressures if the condenser can withstand superheated steam.

550 The isothermal expansion process can not be implemented in practice which is a practical
551 irreversibility of the steam power cycle. A one-stage reheating process is shown in Figure
552 15(a). Assuming that regenerative preheating is not used (the process 5-1 is reversible), the
553 near optimal reheating pressure is obtained by a sensitivity analysis. Figure 15(b) shows how
554 the cycle efficiency varies with the ratio between the reheating pressure (p_{RH1}) and the main
555 steam pressure (p_2). The solid lines represent the cases in which the reheating temperature is
556 equal to the main steam temperature. The dashed lines are for the cases in which the reheating
557 temperature is 20 K higher than the main steam temperature. The numbers on the lines are the
558 isentropic efficiencies (η_{is}) for the steam turbines (assumed to be the same for all turbine
559 stages). The following conclusions can be observed:

560 (1) The maximum cycle efficiency increases by around 0.2% points when the reheating
561 temperature is 20 K higher than the main steam temperature for various turbine
562 efficiencies.

563 (2) The cycle efficiency could be smaller than the value without reheating if the reheating
 564 pressure is too low, since the mean temperature of the heat addition for the reheating
 565 process in such cases is too low.

566 (3) Without reheating, the cycle efficiency is reduced from 53.4% to 46.0% if the turbine
 567 isentropic efficiency decreases from 1.0 to 0.9. The corresponding drop in the thermal
 568 efficiency of the plant is 7.01% points.

569 (4) When the turbine isentropic efficiency is 0.90 (close to state-of-the-art technology), the
 570 optimal pressure ratio between the reheating pressure and the main steam pressure is 0.24.
 571 This optimal value is almost equal to the value (0.237) in the reference plant where
 572 regenerative feedwater preheating is used[5].

573

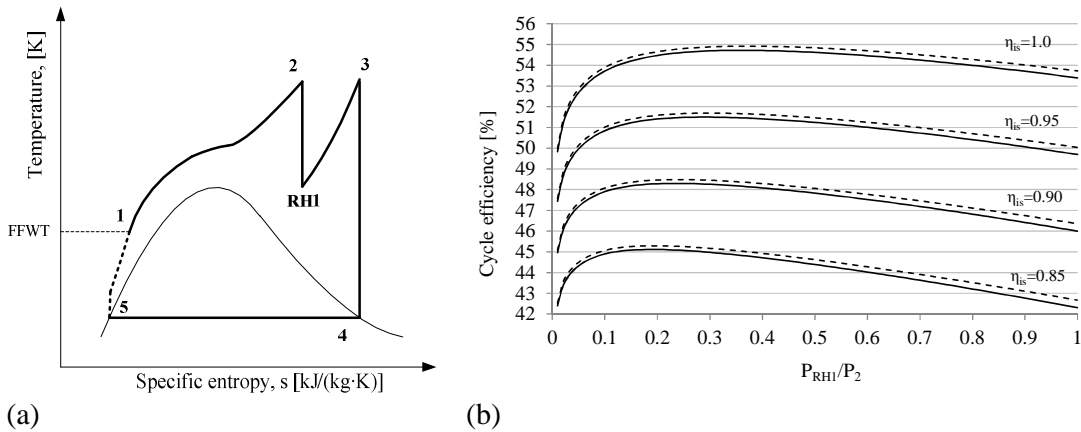


Figure 15 One-stage reheating process: (a) $T-s$ diagram, (b) Cycle efficiency

574

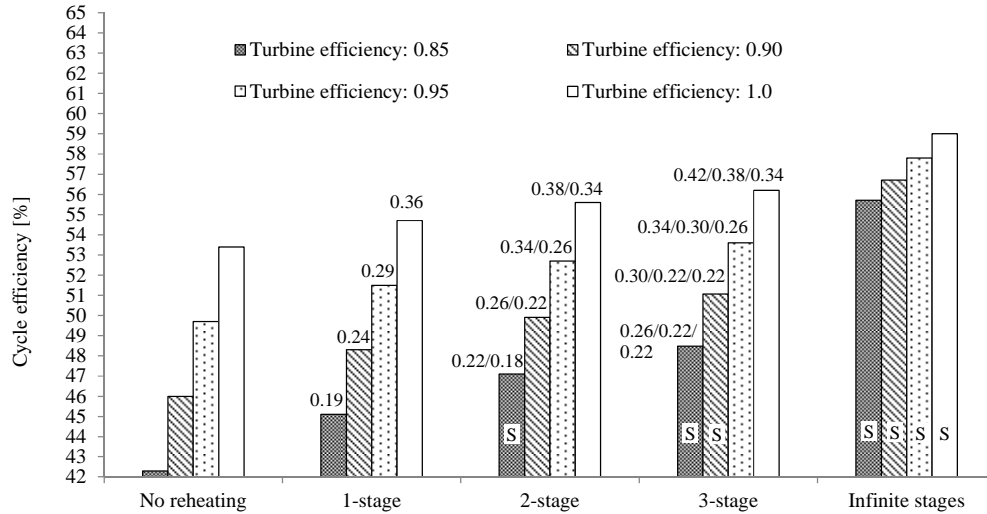


Figure 16 Influence of number of reheating stages on the steam cycle efficiency

575
576
577

Figure 16 shows the influence of the number of reheating stages on the cycle efficiency for different turbine efficiencies. The efficiencies for all the stages are assumed to be the same.

578
579

The reheating temperatures are assumed to be the same as the main steam temperature. The cycle efficiencies are obtained by sensitivity analysis and are thus near optimal values. When

580
581

more than one-stage reheating is applied, the steam from the last stage of the turbine is superheated for some cases (marked as ‘S’ on the bars) in order to get the maximum

582
583

efficiency. The numbers above each bar in the reheating cases (with finite stages) are the optimal ratio of the reheating pressure to the inlet pressure of the upstream turbine.

584
585

Obviously, the improvement in cycle efficiency diminishes with an increasing number of reheating stages. When the turbine efficiency is 0.9, the cycle efficiency increases 2.3% points

586
587

by one-stage reheating, 1.6% points by a second reheating stage and 1.2% points by a third reheating stage. The improvement in cycle efficiency with increasing number of reheating

588
589

stages is more notable with lower turbine efficiencies.

590
591

4.4.4. Other practical limitations on the thermal efficiency

592 In the previous sections, the condensate is assumed to be reversibly brought to the final
593 feedwater conditions. In practice, regenerative heating and pumping are used to lift the
594 temperature and pressure. For modern steam cycles, 8-10 feedwater heaters are commonly
595 used, resulting in very small irreversibilities. The irreversibilities in the feedwater heaters (the
596 deaerator included) and pumps are reported to be responsible for around 1.2% of the thermal
597 input[28, 29]. The same value is assumed for the reference power plant. The steam extraction
598 reduces the irreversibilities in the turbines and the condenser. The condensate flow is around
599 75% of the main steam flow[28, 29]. Thus the irreversibilities in the condenser can be reduced
600 by 1.15% of the thermal input compared to the value presented in Section 4.4.3 (4.6%). Table
601 1 shows the changes in thermal efficiency. When all the components are included, the thermal
602 efficiency is very close to the value for the reference power plant (45.5% as presented in
603 Table A1).

604 **Table 1.** Consequent changes in plant thermal efficiency (%)

Turbine efficiency	1.0	0.95	0.9
Cycle efficiency for one-stage reheating (refer to Figure 13)	54.7	51.5	48.3
Reheating temperature is 20 K above the main steam temperature	54.9	51.7	48.5
Cycle efficiency is converted into thermal efficiency (by a factor of boiler efficiency, 94.7%)	52.0	49.0	45.9
Irreversibilities for the feedwater heating and pumping included	50.8	47.8	44.7
Irreversibilities in the condenser is reduced due to steam extraction	52.0	49.0	45.9
Auxiliary power is included (1.7% of the thermal input[5])	51.3	47.3	44.2

605

606

607 **5. Emissions control: CO₂ capture**

608 Technologies for the control of SO_x, NO_x and particles in thermal power plants are relatively
609 mature. For the reference plant, both low NO_x burners and a selective catalytic reduction
610 (SCR) DeNO_x plant are used for the control of NO_x emissions. The flue gas desulphurization
611 (FGD) unit is assumed to remove 98% of SO_x in the flue gas and finally the electrostatic
612 precipitator (ESP) is used for the removal of particles[5]. The corresponding energy

613 consumption for the control of SO_x, NO_x and particles is small and included in the auxiliary
614 power in Table 1.

615 The control of CO₂ emissions from thermal power plants is a possible measure to mitigate
616 climate change. Various approaches for CO₂ capture are under investigation. They are
617 normally classified into three categories: post-combustion, pre-combustion and oxy-
618 combustion[30]. For post-combustion, the CO₂ is separated directly from the flue gas, thus the
619 main separation is between N₂ and CO₂. For pre-combustion, the fuel is converted into syngas
620 (CO and H₂) by gasification or reforming, then the CO is further converted into CO₂ by the
621 water gas shift reaction, and finally CO₂ is separated from H₂ prior to combustion. Thus the
622 main separation in pre-combustion is between H₂ and CO₂. The key idea of oxy-combustion is
623 to use pure O₂ or other oxidants such as metal oxides (CLC[3]) instead of air for the
624 combustion, resulting in concentrated CO₂ in the flue gas, thus the main separation is between
625 O₂ and N₂.

626 The capture of CO₂ from coal based power plants causes considerable thermal efficiency
627 penalties, typically varying from 6.5 to 15% points (energy consumption for CO₂ compression
628 is included) depending on the technology pathways[30, 31]. There is a minimum energy
629 penalty which is limited by thermodynamics. When a process is assumed to be
630 thermodynamically reversible, the minimum work consumption (or production) is equal to the
631 difference between the exergy of the product streams and the exergy of the feed streams. In
632 the case of reversible removal of CO₂ from the reference plant, the CO₂ is assumed to be
633 directly separated from the flue gas at ambient temperature and is then isothermally
634 compressed to transportation pressure ($p_{\text{transportation}} = 110$ bar, according to literature[5]), as
635 shown in Figure 17. Both separation and compression processes are assumed to be reversible.

636 The minimum work for the separation and compression of CO₂ can be calculated[12], thus the
 637 thermal efficiency including CO₂ capture can be obtained.

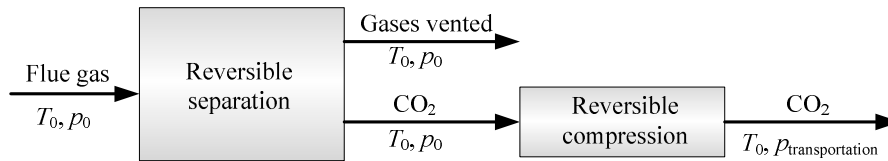


Figure 17 A reversible CO₂ capture process

638
 639
 640

640 Figure 18(a) shows the thermal efficiency for various CO₂ recovery rates (referred to the
 641 numbers for each curve on the figure) at different air factors for the reference power plant.
 642 The purity of the captured CO₂ is assumed to be 1.0. The dashed curves represent cases when
 643 only CO₂ separation work is included, while the solid curves represent cases when both CO₂
 644 separation work and compression work are included. When the CO₂ recovery rate is zero, the
 645 thermal efficiency is actually equal to the value when CO₂ capture is not applied (the
 646 temperature of the flue gas vented is 393 K). The following conclusions can be observed from
 647 Figure 18(a):

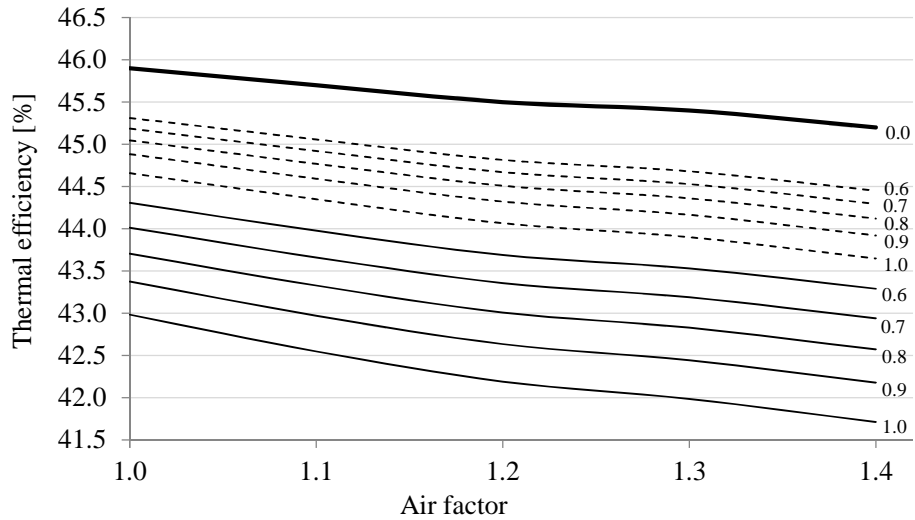
- 648 (1) Within the given range of air factor for a CO₂ recovery rate of 1.0, the thermal efficiency
 649 penalty related to CO₂ capture is 2.92-3.49% points, where the reversible separation of CO₂
 650 contributes 1.24-1.55% points (around 43% of the total penalty).
- 651 (2) Not very surprisingly, an obvious reduction in efficiency penalty can be observed when
 652 the CO₂ recovery rate is reduced. For the reference plant where the air factor is 1.22, the
 653 efficiency penalty related to CO₂ capture reduces from 3.31 to 1.81% points when the CO₂
 654 recovery rate decreases from 1.0 to 0.6. The penalty related to CO₂ separation reduces from
 655 1.43 to 0.69% points. Thus, partial capture of CO₂ in power plants may be attractive when
 656 the investment cost of equipment is taken into consideration[32]. This will depend on the
 657 future cost of emitting CO₂.

658 (3) The changes in efficiency penalty (also in work consumption which is not shown in the
659 figure) with the CO₂ recovery rate become smaller when the recovery rate decreases. The
660 more the recovery rate is decreased, the lower the relative efficiency gain will be. Thus
661 energy saving by reducing the recovery rate should preferably be implemented at high
662 recovery rates.

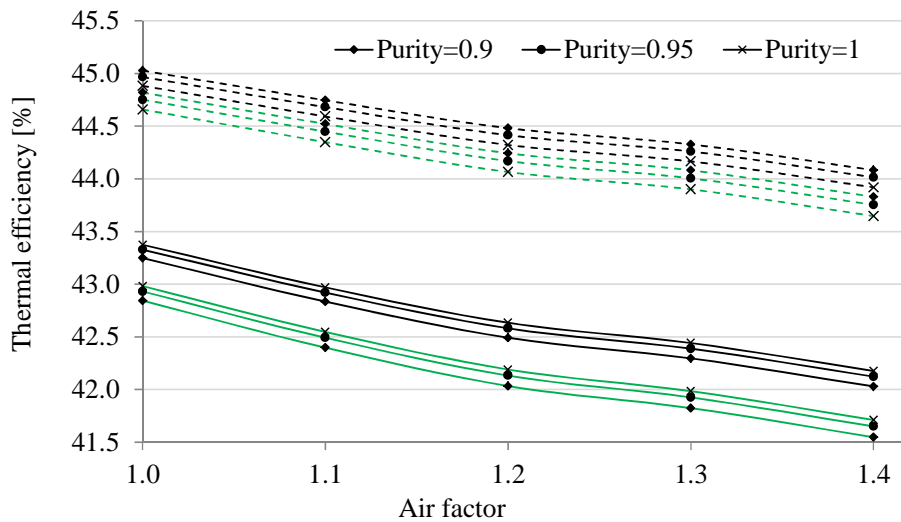
663
664 Figure 18(b) shows the thermal efficiency for different CO₂ purities (mole fraction: 0.9, 0.95
665 and 1.0). Since the main separation is between N₂ and CO₂, the impurity in the captured CO₂
666 is assumed to be N₂. Two recovery rates are investigated: 0.9 and 1.0. The following two
667 conclusions can be made:

668 (1) The thermal efficiency does not change much with the purity of CO₂. For a recovery rate
669 of 1.0, the thermal efficiency increases about 0.15% points at various air factors when the
670 purity of CO₂ increases from 0.9 to 1.0.

671 (2) The separation work increases when the purity of CO₂ increases, however, the
672 compression work decreases since fewer impurities are compressed. According to Figure
673 18(a), the compression work contributes more to the total efficiency penalty than the
674 separation work, thus the total efficiency penalty related to CO₂ capture decreases.
675 Therefore it is more favorable in the reversible case to capture CO₂ with high purity.



(a)



(b)

Figure 18 Thermal efficiency including ideal CO₂ capture processes: (a) various CO₂ recovery rates when the CO₂ purity =1, (b) various CO₂ purities when the CO₂ recovery rate = 1 (curves in green color) and 0.9 (curves in black color).

676

677

678

The above observations from Figures 18(a) and 18(b) are based on the assumption that the

679

capture processes are reversible. The thermal efficiency shown in the two figures are thus

680

theoretical maximum values. Reversible processes are difficult to realize in practice, however,

681

the observations can somewhat guide practical improvement measures of CO₂ capture

682

processes, e.g. the improvement potential by developing advanced solvents such as ion liquids

683 is limited by the minimum energy penalty. For the reference power plant[5], the thermal
 684 efficiency penalty is 11.7% points when a monoethanolamine (MEA) based solvent is used
 685 for capturing CO₂. This value is more than 3 times the theoretical minimum (thermodynamics
 686 limited). The difference is mainly caused by the technology route for CO₂ capture.

687

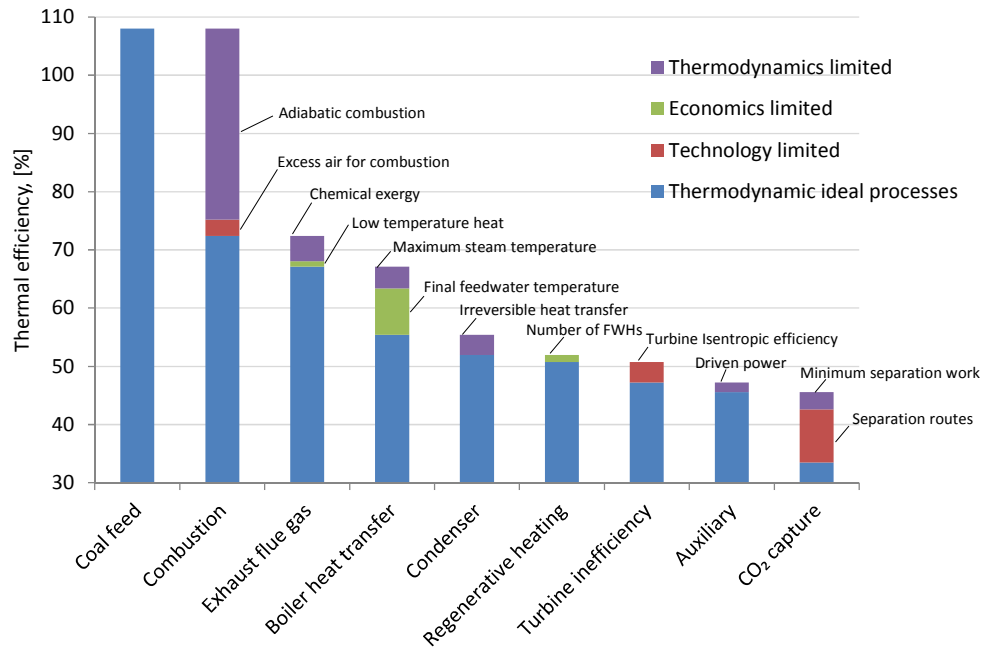


Figure 19 Decrease of the plant thermal efficiency caused by various factors

688

689

690

A summary on the decrease of thermal efficiency from theoretical maximum to practical values

691

for the reference plant is shown in Figure 19. The thermal efficiency is reduced by adding

692

limitations in each unit operation. The dominant factors are listed on the figure and are

693

classified into thermodynamic, technical and economic categories. **The potential for**

694

improvement on in each unit can easily be determined without detailed exergy analysis on the

695

entire power plant. Figure 19 shows that adiabatic combustion of coal is the most inefficient

696

process and thus a technology shift from adiabatic combustion to new oxidation routes such

697

as chemical looping combustion and fuel cells is necessary for significant efficiency

698

improvements. It can also be observed that the technical factors are more dominant than

699 economic factors, thus efforts should focus more on technology development such as reducing
700 air factors for combustion, developing more efficient steam turbines, and exploring advanced
701 separation routes for CO₂ capture. Note that the MEA capture of CO₂ causes the second
702 largest loss of efficiency after combustion irreversibilities. The final boiler feedwater
703 temperature has also caused a considerable reduction in thermal efficiency. This temperature
704 is economics limited that determines the average temperature of heat addition to the steam
705 cycle.

706 **6. Conclusions**

707 A systematic methodology has been presented in this paper for the assessment in efficiency
708 losses for direct combustion coal to power processes step by step and potential means of
709 reducing these losses. The thermal efficiency was decreased to practical values by adding
710 limitations such as thermodynamic, technical and economic factors. The primary advantage of
711 the methodology is that all possible improvement measures can be covered and the
712 improvement potential can be quickly predicted without knowing process details. As an
713 illustrative example, in order to increase the thermal efficiency by 0.1% points for the
714 reference power plant, the following measures can be implemented: (1) reducing the air factor
715 by 0.057, (2) reducing the flue gas temperature by 4.5 K, (3) increasing the final feedwater
716 temperature by 4 K, (4) increasing the main steam temperature by 8 K, and (5) increasing the
717 main steam pressure by 10 bar.

718 The following four observations are directly derived when applying the methodology: (1) the
719 low temperature heat of the flue gas should primarily be recovered by the boiler system before
720 using Organic Rankine Cycles to recover work; (2) when reheating is implemented
721 (particularly for two or more stages), higher thermal efficiency may be achieved if the steam
722 at the outlet of the last turbine stage is superheated; (3) it is concluded that as turbine
723 isentropic efficiency improves, the gain in thermal efficiency from reheating decreases; and

724 (4) the second largest loss after combustion in a coal based power plant with MEA capture of
725 CO₂ is caused by this capture. Hence, the tremendous efforts being spent on developing
726 improved CO₂ capture technologies are indeed justified.

727 The minimum thermal efficiency penalty related to direct CO₂ capture from the flue gas is
728 calculated to be 2.92-3.49% points, where the separation and the compression of CO₂
729 contribute about 43% and 57% respectively. Considerable energy savings can be achieved by
730 decreasing the CO₂ recovery rate, particularly at high recovery rates. The CO₂ is preferably
731 captured at higher purities. Practical limitations on CO₂ capture are subject to further
732 investigations.

733

734 **Acknowledgments**

735 This publication has been produced with support from the BIGCCS Centre, performed under
736 the Norwegian research program Centres for Environment-friendly Energy Research (FME).

737 The authors acknowledge the following partners for their contributions: Gassco, Shell, Statoil,
738 TOTAL, GDF SUEZ and the Research Council of Norway (193816/S60).

739

740 **NOMENCLATURE**

\dot{E}	exergy, kW
e	specific exergy, kJ/kg or kJ/mole
\dot{F}	molar flow, mole/s
f	air factor
\dot{G}	Gibbs free energy, kW
\dot{H}	enthalpy, kW
h	specific enthalpy, kJ/kg or kJ/mole
i	irreversibility, kW

\dot{m}	mass flow, kg/s
p	pressure, bar
\dot{Q}	heat, kW
\bar{R}	universal gas constant, kJ/(mole·K)
\dot{S}	total entropy, kW/K
s	specific enthalpy, kJ/(kg·K)
T	temperature, K or °C
\dot{W}	work, kW
x	molar fraction

Geek Letters

Δ	symbol of differences
η	efficiency
φ	ratio of the chemical exergy to the lower heating value
ω	stoichiometric ratio for combustion

Sub and superscripts

0	reference state
ad	adiabatic
C	combustion; cold end
ch	chemical
eco	economizer
FG	flue gas
fw	feed water
H	hot end
i	component index
is	isentropic
j	phase index
min	minimum
mix	mixing
ms	main steam

ph	physical
pre	preheater
RH	reheating steam
SC	steam cycle
tot	total

Abbreviations

BFW	boiler feedwater
CLC	chemical looping combustion
ESP	electrostatic precipitator
FFWT	final feedwater temperature
FGD	flue gas desulphurization
HHV	higher heating value
HP	high pressure
LHV	lower heating value
LP	low pressure
MS	main steam
ORC	organic Rankine cycle
RH	reheating
S	superheated
SCR	selective catalytic reduction

741

742 Appendix

743 **Table A1.** Main parameters of the reference plant [14]

Parameters	Values
Ambient conditions	288.15 K, 1.01 bar and 60% relative humidity
Main steam (MS)	600.0 kg/s, 270 bar, 873 K
One-stage reheating (RH) steam	485.2 kg/s, 60 bar, 893 K
Feedwater heaters	5 LP heaters and 3 HP heaters
Final feedwater	320 bar, 581 K
Exhaust flue gas	393 K

Condenser pressure	0.048 bar
Gross electrical output	819 MW
Auxiliary power consumption (feedwater pumping is included)	65 MW
Coal feed	65.765 kg/s
Lower heating value (LHV) of coal	25,170 kJ/kg
Thermal input (LHV)	1,655.3 MW
Thermal efficiency (LHV)	45.5%

744

745

746 **Table A2.** Coal characteristics [14]

	As received	Dry
Proximate analysis, %		
Moisture	8.00	0
Volatile matter	22.90	24.9
Ash	14.15	15.4
Fixed carbon	54.90	59.7
Total sulphur	0.52	0.56
Ultimate analysis, %		
Carbon (C)	66.52	72.31
Hydrogen (H)	3.78	4.11
Nitrogen (N)	1.56	1.70
Sulfur (S)	0.52	0.56
Chlorine (Cl)	0.01	0.01
Ash	14.15	15.38
Moisture (H ₂ O)	8.00	0
Oxygen (O)	5.46	5.93
High heating value (HHV), kJ/kg	26,230	28,500
Low heating value (LHV), kJ/kg	25,170	27,573
Chemical exergy, kJ/kg	27,295	
Stoichiometric air/coal ratio	8.8122	

747

748 **Table A3.** Compositions of atmospheric air

Component	Volume fraction (dry)	Volume fraction at 60% relative humidity
N ₂	78.09	77.3
CO ₂	0.03	0.03

H ₂ O	0	1.01
Ar	0.93	0.92
O ₂	20.95	20.74

749

750

751 **REFERENCES**

- 752 [1] International Energy Agency, World Energy Outlook 2014.
- 753 [2] G.J. Silvestri, R.L. Bannister, T. Fujikawa, A. Hizume. Optimization of advanced steam condition
754 power plants. *J Eng Gas Turbines Power*. 114 (1992) 612-20.
- 755 [3] N.R. McGlashan. Chemical-looping combustion - a thermodynamic study. *Proc IMechE, Part C: J*
756 *Mechanical Engineering Science*. 222 (2008) 1005-19.
- 757 [4] G. Angelino, C. Invernizzi. Binary and ternary liquid metal - steam cycles for high-efficiency coal
758 power stations. *Proc IMechE, Part A: J Power and Energy*. 220 (2006) 195-205.
- 759 [5] H. Spliethoff. Power generation from solid fuels. Springer-Verlag Berlin Heidelberg, Berlin,
760 Heidelberg, Germany, 2010.
- 761 [6] A. Bejan. Advanced engineering thermodynamics. 2nd ed. John Wiley & Sons, New York, US,
762 1997.
- 763 [7] M.M. El-Wakil. Powerplant technology. McGraw-Hill, New York, US, 2002.
- 764 [8] J.K. Salisbury. Steam turbines and their cycles. John Wiley & Sons, New York, US, 1950.
- 765 [9] Y.A. Cengel, M.A. Boles. Thermodynamics: an engineering approach. 6th ed. McGraw-Hill, New
766 York, US, 2006.
- 767 [10] M.J. Moran, H.N. Shapiro, D.D. Boettner, M.B. Bailey. Principles of engineering
768 thermodynamics. 7th ed. John Wiley & Sons, New Jersey, US, 2012.
- 769 [11] C. Fu, R. Anantharaman, K. Jordal, T. Gundersen. Thermal efficiency for coal to power: from
770 theoretical to practical assessments. The 26th International Conference on Efficiency, Costs,
771 Optimization, Simulation and Environmental Impact of Energy Systems (ECOS 2013), Guilin, China,
772 July 2013.
- 773 [12] R. Anantharaman, K. Jordal, T. Gundersen. CO₂ capture processes: novel approach to
774 benchmarking and evaluation of improvement potentials. *Energy Procedia*. 37 (2013) 2536-43.
- 775 [13] H.M. Kvamsdal, K. Jordal, O. Bolland. A quantitative comparison of gas turbine cycles with
776 capture. *Energy*. 32 (2007) 10-24.
- 777 [14] Franco F, Anantharaman R, Bolland O, Booth N, van Dorst E, Ekstrom C, Fernandes ES, Macchi
778 E, Manzolini G, Nikolic D, Pfeffer A, Prins M, Rezvani S, Robinson L. European Best Practice
779 Guidelines for Assessment of CO₂ Capture Technologies. European Benchmarking Task Force, 2011.
780 Available at: <http://www.energia.polimi.it/news/D%204_9%20best%20practice%20guide.pdf>
781 [accessed 17.04.2015].
- 782 [15] T.J. Kotas. The exergy method of thermal power plant analysis. Exergon Publishing Company,
783 London, UK, 2012.
- 784 [16] J. Szargut. Exergy method: technical and ecological applications. WIT Press, Southampton, UK,
785 2005.
- 786 [17] R.C. Flagan, J.H. Seinfeld. Fundamentals of air pollution engineering. Prentice-Hall, New Jersey,
787 US, 1988.
- 788 [18] A.J. Appleby, F.R. Foulkes. Fuel cell handbook Van Nostrand Reinhold, New York, US, 1989.
- 789 [19] A.E. Lutz, R.S. Larson, J.O. Keller. Thermodynamic comparison of fuel cells to the Carnot cycle.
790 *Int J Hydrogen Energy*. 27 (2002) 1103-11.
- 791 [20] W.R. Dunbar, N. Lior. Sources of combustion irreversibility. *Combust Sci and Tech*. 103 (1994)
792 41-61.
- 793 [21] M.J. Prins, K.J. Ptasinski. Energy and exergy analyses of the oxidation and gasification of carbon.
794 *Energy*. 30 (2005) 982-1002.
- 795 [22] M.M. Hossain, H.I. de Lasa. Chemical-looping combustion (CLC) for inherent separations - a
796 review. *Chemical Engineering Science*. 63 (2008) 4433-51.

- 797 [23] C. Fu, T. Gundersen. Exergy analysis and heat integration of a coal-based oxy-combustion power
798 plant. *Energy & Fuels*. 27 (2013) 7138-49.
- 799 [24] A.A. Lakew, O. Bolland. Working fluids for low-temperature heat source. *Appl Therm Eng*. 30
800 (2010) 1262-8.
- 801 [25] A.I. Kalina. Combined cycle system with novel bottoming cycle. *J Eng Gas Turbines Power*. 106
802 (1984) 737-42.
- 803 [26] R.W. Haywood. A generalized analysis of the regenerative steam cycle for a finite number of
804 heaters. *Proc IMechE*. 161 (1949) 157-64.
- 805 [27] A. Seltzer, Z. Fan, H. Hack. A method to increase oxyfuel power plant efficiency and power
806 output. The 37th International Technical Conference on Clean Coal & Fuel Systems, Clearwater,
807 Florida, US, June 2012.
- 808 [28] I. Dincer, M.A. Rosen. *Exergy: energy, environment and sustainable development*. Elsevier,
809 Amsterdam, Netherlands, 2007.
- 810 [29] Y. Yang, L. Wang, C. Dong, G. Xu, T. Morosuk, G. Tsatsaronis. Comprehensive exergy-based
811 evaluation and parametric study of a coal-fired ultra-supercritical power plant. *Applied Energy*. 112
812 (2013) 1087-99.
- 813 [30] J. Davison. Performance and costs of power plants with capture and storage of CO₂. *Energy*. 32
814 (2007) 1163-76.
- 815 [31] M. Kanniche, R. Gros-Bonnivard, P. Jaud, J. Valle-Marcos, J.-M. Amann, C. Bouallou. Pre-
816 combustion, post-combustion and oxy-combustion in thermal power plant for CO₂ capture. *Applied*
817 *Thermal Engineering*. 30 (2010) 53-62.
- 818 [32] A.N. Hildebrand, H.J. Herzog. Optimization of carbon capture percentage for technical and
819 economic impact of near-term CCS implementation at coal-fired power plants. *Energy Procedia*. 1
820 (2009) 4135-42.